Progressive impairment of directional and spatially precise trajectories by TgF344-AD Rats in the Morris Water Task

Laura E. Berkowitz, Ryan E. Harvey, Emma Drake, Shannon M. Thompson, Benjamin J. Clark

Department of Psychology, University of New Mexico, Albuquerque, New Mexico

Key Words: dementia, disorientation, spatial behavior, spatial memory, hippocampus, limbic

To whom correspondence should be addressed:

Benjamin J Clark, Ph.D.

email: bnjclark@unm.edu

Abstract

Spatial navigation is impaired in early stages of Alzheimer's disease (AD), and may be a defining behavioral marker of preclinical AD. Nevertheless, limitations of diagnostic criteria for AD and within animal models of AD make characterization of preclinical AD difficult. A new rat model (TgF344-AD) of AD overcomes many of these limitations, though spatial navigation has not been comprehensively assessed. Using the hidden and cued platform variants of the Morris water task, a longitudinal assessment of spatial navigation was conducted on TgF344-AD (n=16) and Fischer 344 (n=12) male and female rats at three age ranges: 4 to 5 months, 7 to 8, and 10 to 11 months of age. TgF344-AD rats exhibited largely intact navigation at 4-5 and 7-8 months of age, with deficits in the hidden platform task emerging at 10-11 months of age. In general, TgF344-AD rats displayed less accurate swim trajectories to the platform and a wider search area around the platform region compared to wildtype rats. Impaired navigation occurred in the absence of deficits in acquiring the procedural task demands or navigation to the cued platform location. Together, the results indicate that TgF344-AD rats exhibit comparable deficits to those found in individuals in the early stages of AD.

Introduction

Alzheimer's disease (AD) is the most common form of dementia in the United States and is characterized by progressive cognitive decline and neurodegeneration (Association and others, 2017). AD pathology, marked by amyloid plaques and neurofibrillary tangles that accumulate throughout the limbic system and hippocampus, is predicted to initiate up to 20 years prior to the onset of behavioral symptoms (Gao et al., 1998; Mielke et al., 2014). Although the long preclinical period poses a significant challenge to early diagnosis of AD (Dubois et al., 2016; Graham et al., 2017) subtle changes in memory, as observed in amnestic mild cognitive impairment (aMCI), can indicate an increased risk of progressing to dementia (Petersen, 2004; Winblad et al., 2004). However, because not all cases of aMCI progress to AD, there is a growing need for sensitive behavioral assessments for AD diagnosis.

Mounting evidence suggests that spatial disorientation, sometimes referred to as wandering, are among the earliest memory complaints in AD (Bianchini et al., 2014; Bird et al., 2010; Chan et al., 2016; Guariglia and Nitrini, 2009; Pai and Jacobs, 2004; Yew et al., 2013). In general, disorientation is characterized as deficient localization of hidden goals (Hort et al., 2007), a loss of direction sense (Cushman et al., 2008; deIpolyi et al., 2007; Monacelli et al., 2003; Tu et al., 2015), or an impairment in correctly identifying familiar spatial scenes after a small change in view-point (Bird et al., 2010; Chan et al., 2016). Deficits in establishing or utilizing map-like (allocentric) frameworks for navigation are frequently linked with the earliest stages of AD, while later stages are associated with deficits in simpler forms of navigation, such as approaching cues, or utilizing egocentric movements to guide behavior (Hort et al., 2007). Navigation can

therefore serve as an early marker of AD, with some studies indicating that disoriented patients are more likely to convert from aMCI to an AD diagnosis (Bird et al., 2010; Laczó et al., 2009).

Animal models have been utilized to better understand spatial disorientation in AD, however most fail to produce the full spectrum of amyloid and tau dysfunction (Do Carmo and Cuello, 2013; LaFerla and Green, 2012). A recent rat model of AD, called the TgF344-AD rat, has been developed to express both the Swedish form of mutant amyloid precursor protein gene and human mutant presenilin 1 and progressively develop a comprehensive profile of AD pathology (Cohen et al., 2013). Importantly, TgF344-AD rats display characteristic plaque and tangle pathogenesis, as well as neuroinflammation, and neurovascular dysfunction resulting in substantial cell loss (Joo et al., 2017). Elevated amyloid, tau, and activated microglia pathology can be detected within both the entorhinal cortex and hippocampus at 6 months of age, and by 16 months of age, the expression of amyloid and tau increase substantially (Cohen et al., 2013; Rorabaugh et al., 2017). A recent study has reported that reductions in the strength of excitatory transmission can be detected at entorhinal-to-dentate gyrus synapses as early as 6 months (Smith and McMahon, 2018). These synaptic changes precede reductions in neurotransmission at CA3-CA1 hippocampal synapses, which begin around 9 months of age. This emerging pattern of pathogenesis and altered signaling along the Trisynaptic circuit is consistent with the human condition (Braak and Braak, 1995; Thal et al., 2002).

Currently, only a small number of studies have investigated the time-course of spatial navigation impairment in the TgF344-AD rat model (Cohen et al., 2013; Pentkowski et al., 2017; Rorabaugh et al., 2017). While experiments have determined

93 that spatial deficits can be detected after 15 months of age (Cohen et al., 2013;
94 Rorabaugh et al., 2017; Voorhees et al., 2017), the onset of navigation impairment has
95 been less clear. Some studies have reported that TgF344-AD rats are largely unimpaired
96 in navigating to a fixed hidden goal location between 4 and 6 months of age (Cohen et
97 al., 2013; Pentkowski et al., 2017), while others have reported deficits at 6 months of age
98 (Rorabaugh et al., 2017). The variability between studies could be related to subtle
99 differences in performance by male and female TgF344-AD rats, which are often pooled
100 into a single group. Sex differences in spatial behavior in AD have been reported in other
101 rodent models of AD (Clinton et al., 2007; Granger et al., 2016; Mielke et al., 2014), and
102 is additionally supported by the fact that females exhibit a disproportionally higher rate of
103 progression to AD and increased severity of clinical dementia. Further, given the cross-
104 sectional design of previous studies, and the fact that TgF344-AD display differing
105 locomotor behaviors as early as 6 months of age (Cohen et al., 2013), non-spatial
106 variables associated with procedural learning could also play a role.
107 The overall aim of the present study was to characterize spatial navigation in
108 TgF344-AD rats at early stages of development. A longitudinal design was employed to
109 capture compensatory behaviors possibly secondary to burgeoning pathology (Morganti
110 et al., 2013) and to control for age-effects commonly attributed with procedural task
111 demands (van Groen et al., 2002; Vicens et al., 2002). Both male and female subjects
112 were tested at three age ranges starting from 4 to 5 months, 7 to 8 months, and 10 to 11
113 months in the hidden and cued platform variants of the Morris water task (Harker and
114 Whishaw, 2002; Morris, 1984; Pentkowski et al., 2017; Vorhees and Williams, 2006).
115 Several standard measures were used to describe the performance and spatial distribution

of movements in the pool, including escape latency, path length, and platform proximity. However we also provided an assessment of directional disorientation by quantifying the proportion of direct swims toward the platform region at each age of testing (Garthe et al., 2009; Gehring et al., 2015). Finally, a convolution analysis was employed to determine how switching to direct swims or becoming more efficient at less direct swims contributes to task performance. Consistent with what has been reported in human AD, we hypothesized that rats would express age-dependent impairments in the accuracy of their swim trajectories in the hidden platform variant of the Morris water task. We additionally hypothesized that these impairments would be expressed independent of motor and procedural deficits, and co-occur with intact acquisition of cued platform learning.

Methods

Subjects

Sixteen TgF344-AD (Tg) rats counterbalanced for sex and expressing mutant human amyloid precursor protein (APPsw) and presenilin 1 (PS1ΔE9) were obtained directly from the Rat Resource & Research Center (Columbia, MO). Twelve wild type Fischer 344 (WT) rats (Harlan laboratories, Indianapolis, IN) counterbalanced for sex served as control subjects. Subjects were maintained under controlled temperature (21 ± 2 ◦C), were housed with Tg or WT pairs, and were kept on a 12 hour light/dark cycle (lights off at 09:00 AM). Food and water was provided *ad libitum* throughout the duration of the study. Animal care practices and experiments were approved by the University of New Mexico Institutional Animal Care and Use Committee and adhered to

the APA ethical principles of animal use.

Longitudinal Design

A longitudinal mixed design was used to assess changes in navigation in the hidden and cued platform variants of the Morris water tasks at three age time-points. Subjects were placed into groups by genotype (Tg or WT) and further grouped by sex (male or female). At the start of testing, subjects' age ranged from 4.30-5.7, 7.5-8.9, and 10.3-11.7 months at each respective time point. For clarity, we refer to these ages throughout the remaining manuscript as, 4-5 months, 7-8 months, and 10-11 months of age. Tasks were administered in the same temporal order at each time point (Fig. 1A), whereby the hidden platform task was administered before cued platform training. Procedures were maintained between time points and experimenters did not change throughout the duration of the study. All rats were naïve to experimentation prior to the start of the first experiments at 4 months of age.

Apparatus and Testing Room

A circular pool (150 diameter, 48 cm high) with a white inner wall situated on a wooden frame (50 cm high) and a 16 cm x 16 cm plastic escape platform covered with a metal grate with a height of 25cm was used for all tasks. The pool was filled with water (20 - 22°C) until the level reached ~2.5 cm above the top of the platform. Non-toxic white paint (~500 ml) was used to make the water opaque. Distal environmental cues were composed of various objects (movie posters, thin particle board hangings) and furniture (desks & bookshelves) and were maintained in fixed locations during training at

each time-point. However, the cues, cue layout, pool, and platform location was modified at each time-point (Fig. 1B). An overhead camera was fastened above the pool to record swim behavior for subsequent analysis.

Morris Water Task - Hidden Platform

The purpose of the hidden platform variant of the Morris water task is to assess animal navigation to a precise spatial location based on multiple allocentric spatial cues particularly those associated with the features of the distal environment (Clark et al., 2015; Harker and Whishaw, 2002; Morris, 1984; Vorhees and Williams, 2014). Rats were given 4 trials per day for 5 consecutive days. An individual trial was composed of randomly placing the rat into the pool at one of four equidistant drop locations facing the wall. Once the platform was found, the subject remained on the platform for 10 seconds. Drop location varied between time point/trials/days, but was maintained between subjects. At the end of the trial, the rat was returned to a holding cage, during which time the remaining rats in the cohort were tested (10-20min duration). Subjects were run in groups of seven for each task. At the end of the 4 trials, rats were returned to their home cages in the colony room and the same procedure was repeated the next day. Time to reach the platform was recorded by an experimenter at the end of each trial. The mean escape latencies (seconds) for each animal were calculated for each day (every 4 trials).

No-Platform Probe Test

After 5 days of training in the hidden platform task, a probe trial was conducted in which the platform was removed from the swimming pool. The probe trial was conducted 24 hours after the final trial of the fifth training day. The probe trial was composed of

186 releasing rats from the side of the pool opposite the platform. Rats were permitted to
187 swim for a total of 60 seconds. After the probe test, rats were removed from the pool and
188 placed in a holding cage.
189
190 **Morris Water Task - Cued Platform**
191 A cued-platform test was performed to verify that animals could navigate toward
192 a cue directly associated with the platform location (Clark et al., 2013; Clark and Taube,
193 2009; Morris, 1984). In this task, a 10 cm diameter black ball with a white horizontal
194 stripe was attached to a metal rebar and placed above the center of the platform (11.5 cm
195 above the water). The cue was visible from any location in the pool. Subjects were
196 trained for a single day consisting of 8 trials. Again, a trial consisted of placing a rat by
197 hand into the water facing the wall of the pool at 1 of the 4 starting positions (trial length
198 60 sec; time on platform 10 sec). If the platform was not found within 60 seconds, the
199 experimenter guided the subject to the platform by hand. Time to reach the platform was
200 recorded by an experimenter at the end of each trial.
201
202 **Behavioral Analysis**
203 From the video records, behavioral coders blind to experimental group manually
204 tracked each animal's location in the pool. Tracking and analysis was performed for each
205 trial of the hidden platform, no-platform probe, and cued platform experiments (Clark et
206 al., 2015; Pentkowski et al., 2018). First, raw video files were converted to JPEG images
207 in a Linux bash shell using FFMPEG (https://www.ffmpeg.org). Image files were then
208 imported into Fiji (https://imagej.nih.gov/ij/) and x- y- coordinates of the animal's nose

209 was acquired for each video frame (10 frames/sec) using the Manual Tracking plugin.
210 Custom Matlab (R2017, The MathWorks, Natick, MA) scripts were designed to smooth
211 the tracked swim paths using the runline function from the Chronux toolbox
212 (www.chronux.org). The smoothed paths were then analyzed for path length (cm), swim
213 speed (cm/sec), platform proximity (cm), and search area. Platform proximity was
214 measured by summing the distance between the subject's location and the center of the
215 platform location over 1 sec intervals (Gallagher et al., 1993). The distance from the drop
216 location to the center of the platform was then subtracted from the total summed
217 distances as drop locations were variably distant to the platform. Search area was
218 obtained by first dividing the pool surface into a matrix of 50 x 50 bins (each bin = 3cm x
219 3cm). Search area was expressed as the proportion of the pool visited by the animal
220 (number of visited bins divided by the total number of bins in the matrix).

221 For no-platform probe trials, the pool was divided into four equal quadrants and
222 the total dwell time in each quadrant was determined. From these measures, a platform
223 preference score was calculated by taking the average difference in dwell time between
224 the platform quadrant and the opposite quadrant (Harker and Whishaw, 2002). We also
225 calculated an average platform proximity for the probe test by taking an average of the
226 distance between the subject's location and the center of the platform location across the
227 60 second probe test.

228 Additionally, we performed a detailed swim trajectory analysis to determine the
229 number of directed swim movements toward the hidden platform during training (Brody
230 and Holtzman, 2006; Garthe et al., 2009; Gehring et al., 2015; Graziano et al., 2003;
231 Ruediger et al., 2012; Stone et al., 2011; Wolfer and Lipp, 2000) Briefly, a custom

Matlab script automatically segmented whole paths into 200 cm increments that overlapped 70% to minimize labelling bias secondary to segment start/end points in order to capture the use of various movement types within a given trial (Gehring et al., 2015). An expert coder blinded to group manually categorized the path segments into 11 movement subtypes based on previous work (Garthe et al., 2009; Gehring et al., 2015). For clarity of analysis, the movements were further divided into 4 broad categories. Figure 4 provides a description of each movement subtype and analysis category. Briefly, target-direct movements included trajectories that contained no looping and path lengths less than 200cm and were further defined as a direct movement to platform (i.e. direct) or meandering/arched movements towards platform (i.e. circuitous-direct). Target-indirect movements included circling or searching next to the platform (i.e. target-search), and trajectories that passed by platform (i.e. target-scanning). Spatial-indirect movements involved patterns indicative of spatial processing but were not directed towards the platform location, such as maintaining a swim path set approximately the distance of the platform to the wall (i.e. chaining), searching of a focal area in the pool (i.e. focused-search), sustained swimming in the center of the pool (scanning), and sweeping swim paths traversing pool quadrants (i.e. scanning-surrounding). Non-Spatial movements including wall hugging (i.e. thigmotaxis), using the wall to head in a random trajectory away from the pool wall (i.e. incursion), and a path that circle over itself (i.e. looping). If a segment displayed characteristics of multiple movement types, the path was labeled with all applicable types.

Lastly, an experimenter blind to group quantified the number of non-spatial learning errors during training trials for the hidden platform experiment. As previously

255 described (Harker and Whishaw, 2002; Saucier et al., 1996; Saucier and Cain, 1995),
256 non-spatial errors included diving behavior (diving below the surface of the water during
257 a trial), floating (the absence of swimming for more than 3 sec), platform deflections (the
258 failure to obtain purchase onto the platform after contact), mounting errors (the failure to
259 climb the platform after 1 sec of contacting the platform), and jumping off the platform.
260 Each error was assigned a score of 1 and a total was obtained by summing the errors
261 (Harker and Whishaw, 2002)
262
263 **Statistical Analysis**
264 Statistical analyses were performed using SPSS version 26 (IBM, Armonk, NY)
265 and MATLAB. Mixed model ANOVAs were used to assess differences within or
266 between time points. Between-subject factors consisted of sex (female, male) and
267 genotype (Tg, WT). Outcome measures were evaluated in blocks of four trials (day 1,
268 day 2, day 3, day 4, day 5) or time-point. Log transformations were applied to data that
269 did not meet the assumption of normality. A Greenhouse-Geisser correction was applied
270 to data that did not meet the assumption of sphericity. Two-way ANOVAs were used to
271 compare performance on the cued platform task within a time point using genotype and
272 sex as between subject factors. The results of the detailed path analyses were subjected to
273 Chi square tests. Robust linear regressions using a Tukey's bisquare weight function to
274 minimize the effect of outliers were used to determine the proportion of variance of task
275 performance accounted for by convolved factors (described further in the Results
276 section). Both significant ($p < .05$) and trending non-significant (n.s.) ($.1 > p > .05$) results
277 are reported.

Results

One subject was excluded from the analyses at 10-11 months of age after developing glaucoma. Furthermore, one subject died during testing at 10-11 months of age and thus was not included in the analysis below.

Hidden Platform Task

Swim Latency. Figure 2A displays measures of escape latency for groups at each time-point. On average, animals in all groups showed a progressive decrease in escape latency at each age of testing, indicating that subjects could learn the location of the platform. This observation is supported by a significant day effect for all groups at the three time-points ($Fs \geq 15.25$, $ps \leq .001$). While there were no significant genotype or sex differences at 4-5 and 7-8 months of age, swim duration by Tg rats at 10-11 months of age was appreciably greater than WT animals. This was confirmed by a significant genotype difference in escape latency at the final time-point ($F(1, 23)=5.76$, $p=.025$). In addition, at 10-11 months of age, there was a trend in which Tg females had greater escape latencies relative to all other groups ($\leq$8.1s, $\pm \leq$1.1 sec; $F(1, 23)=3.10$, $p=.092$).

Path Length. Measures of path length mirrored that of escape latency in showing that animals reduced the length of their swims during training at each time-point (Fig. 2B). Again, a mixed ANOVA indicated significant day effects for all groups at the three time-points ($Fs \geq 15.01$, $ps \leq .001$). Sex differences in swim length were detected at 4-5 months of age ($F1, 24) =4.69$, $p=.040$), but not at 7-8 or 10-11 months of age. Although there were no genotype differences at 4-5 and 7-8 months of age, Tg rats had significantly longer paths by 10-11 months ($F (1, 23)=5.18$, $p=.032$).

Spatial Distribution of Swim Paths. The greater path length displayed by Tg rats at 10-11 months of age may reflect a pattern of behavior in which movements are restricted to specific non-platform locations or distributed over wide areas of the pool. To better understand the spatial distribution of swim paths during hidden platform training, we analyzed the overall search area and the relative proximity to the platform of swim paths during each training trial (Fig. 3). ANOVAs conducted on search area and platform proximity indicated a significant day effect at each age ($Fs \geq 30.72$, $ps \leq .001$), however there was no evidence of a significant genotype or sex difference at 4-5 or 7-8 months of age. Nonetheless, Tg rats displayed wider search distances relative to the platform at 10-11 months (Fig. 3A). The observation is supported by significant genotype (F (1, 23)=5.75, p=.025) and genotype by day effects (F(4, 92)=2.58, p=.043). Similarly, Tg rats displayed a search area that was wider compared to WT animals at 10-11 months of age (Fig. 3B). This difference was confirmed by a significant ANOVA for genotype at 10-11 months (F(1, 23)=4.69, p=.041). Collectively, these findings indicate that the swim behavior of Tg rats was less confined to the platform region and distributed to wider regions of the pool.

Swim Trajectory Analysis. In well trained control animals, swim trajectories are typically composed of movements characterized by direct paths beginning at the start point and ending at the platform location. The findings summarized in the sections above suggest that 10-11-month-old Tg rats may express fewer of these directed swims. To address this possibility, we classified swim paths into 11 movement categories (Fig. 4). These swim movements were then merged into 4 categories based on their directedness to the platform (target-direct), a lack of directedness but proximity to the platform (target-

indirect), or a tendency to organize movements in non-platform locations (spatial-indirect), or in a random search (non-spatial).

Figure 5 and 6 show the proportion of each movement category for groups across the three experimental ages and testing days. As expected, both Tg and WT rats displayed an increasing number of direct trajectories as a function of training day at each age (Fig. 6A). However, the overall proportion of target-direct trajectories by Tg rats was significantly lower at 10-11 months of age ($X^2(1) = 12.43$, $p<.001$). Interestingly, the proportion of direct trajectories by female Tg rats was appreciably lower compared to all other groups ($X^2s \geq 5.96$, $ps \leq .014$). Additionally, inspection of target-direct trajectories at earlier ages suggest that Tg rats made fewer of these movements relative to WT animals. Indeed, group comparisons reached significance at 7-8 months of age ($X^2(1) = 5.82$, $p=.015$), and although group differences were not significantly different at 4-5 months of age, Tg females made fewer target-direct trajectories compared to WT females ($X^2(1) = 4.07$, $p=.043$). Together, these results support the conclusion that Tg rats make less directionally precise movements at 7-8 and 10-11 months of age, with a significantly lower proportion of these movements by female Tg rats.

The reduced frequency of target-direct paths by Tg rats suggest that other movements, including those directed near the platform (target-indirect) or in other non-platform locations (spatial-indirect and non-spatial), may be favored by Tg animals (Fig. 6B-D). Consistent with this hypothesis, Tg rats were found to express a greater proportion of target-indirect movements at 10-11 months of age ($X^2(1) = 5.93$, $p=.015$). Furthermore, with respect to target-indirect movements, there was a clear sex difference with Tg males showing a significantly greater proportion of these paths relative to all

other groups ($X^2s \geq 6.75$, $ps \leq .009$). Interestingly, this finding was apparent at 4-5 months, however; at that age Tg females had a greater proportion of target-indirect paths relative to all other groups ($X^2s \geq 6.82$, $ps \leq .009$). Additionally, Tg rats performed a greater number of spatial-indirect trajectories ($X^2(1) = 14.31$, $p < .001$) and fewer non-spatial movements at 10-11 months ($X^2(1)=14.61$, $p \leq .001$). In sum, the reduced frequency of direct trajectories by Tg rats at 10-11 months of age corresponds with an increase in spatially restricted swim paths near the platform location (target-indirect) or in other pool locations (spatial-indirect).

Convolution Analysis. Collectively, the results described in the previous sections indicate that while general performance measures decreased across testing days, group differences were detected at 10-11 months of age. Tg rats expressed fewer direct trajectories toward the platform location at 10-11 months, and at earlier testing ages, suggesting that they utilized other movements to navigate to the platform locations. In other words, it is possible that repeated spatial training and procedural learning may have allowed Tg animals to utilize less-direct strategies that result in similar performance on standard measures. For example, an animal may become better at estimating the distance of the platform to the pool wall (i.e. chaining) over time. Thus, this movement may result in progressively shorter paths to the platform.

Given Tg rats perform a lower proportion of directed movements (either target-direct or target-indirect movements) at 10-11 months, we tested the hypothesis that Tg rat performance is more highly explained by becoming more efficient at non-direct movements rather than switching between non-direct to direct movement categories. To evaluate this hypothesis we utilized a convolution analysis (Brody and Holtzman, 2006;

370 Garthe et al., 2009), which determines whether a change in the frequency of movement
371 subtypes, or a change in the efficiency of swim movements, predicts trial path length
372 (Fig. 7). First, an estimate of the frequency of each movement was calculated by dividing
373 the number of movements in each category by the total number of path segments (Fig.
374 7B). Second, we estimated the efficiency of a given movement by multiplying the
375 frequency of that movement during a trial by the trial path length. Thus, efficiency scores
376 for a given movement subtype reflects the contribution by that movement to trial path
377 length. Two models allowed us to assess the power of changes in efficiency or changes in
378 frequency of movement subtypes in predicting trial path length. Changes in efficiency
379 (ΔEff) scores were derived by keeping frequency constant across trials whereas changes
380 in frequency (ΔFreq) scores were derived by keeping efficiency constant across trials
381 (Fig 7C). Overall values for efficiency (i.e. average efficiency across all 20 trials) and
382 frequency (i.e. frequency of each strategy across all 20 trials) were used as constants.
383 Predicted path length therefore reflects the contribution of the non-constant factor on the
384 trial path length (Fig 7D).

385 Figure 8 summarizes the regression results which indicate that switching between
386 movement categories and becoming efficient at swim movements is significantly
387 predictive of trial path length for all animals. However, switching between movements
388 takes up 27% less of the variance for Tg males and 16% less of the variance for Tg
389 females relative to WT males and WT females, respectively (Fig. 9). Interestingly, Tg
390 male and females exhibited differences in the predictive power of each factor.
391 Specifically, at 10-11 months, switching between movements is a stronger predictor of
392 performance for Tg males (β=4.12, $t(18)$=4.406, p<.001) relative to Tg females (β=1.77,

393 $t(18)=4.36$, $p<.001$). Furthermore, although changes in efficiency take up a larger
394 proportion of the variance for task performance in Tg females relative to Tg males (67%
395 versus 45%, respectively), changes in efficiency hold less predictive weight for Tg
396 females ($\beta=.993$, $t(18)= 5.72$, $p<.001$) relative to Tg males ($\beta=1.80$, $t(18)= 3.67$, $p<.001$).
397 Overall, these results indicate that the performance of Tg animals is less associated with
398 switching between movement categories than WT animals, supporting our hypothesis
399 that Tg animals are more likely the improve the efficiency of their movements than
400 switch to more direct trajectories.

401 *Swim speed and Non-Spatial Errors.* To determine whether the impairments
402 described above might be influenced by deficits in acquiring the task procedures and
403 sensorimotor behavior, we acquired measurements of swim speed during each training
404 trial (Fig. S1). On average, swim speeds increased as a function of test day within each
405 time-point ($Fs\geq 4.20$, $ps\leq.02$). In addition, female rats exhibited faster swim speeds
406 compared male rats—an observation that was consistent at each time-point ($Fs\geq 15.67$,
407 $ps\leq.001$). Nevertheless, there were no significant transgenic differences as Tg and WT
408 animals demonstrated similar swim speeds at 10-11 months of age.

409 We also analyzed the number of non-spatial errors per rat at each age point. The
410 number of errors were summed across days to produce a non-spatial error score (Harker
411 and Whishaw, 2002). Overall, animals in both groups displayed near zero non-spatial
412 error scores at each age of testing (Fig. S2). By 10-11 months of age, only half of the
413 animals in each group expressed 1 or 2 errors over the 5 days of hidden platform testing,
414 indicating an absence of procedural learning deficits in the Tg group ($X^2(2)= 7.54$,

415 p=.37). Thus, given the absence of clear group differences in non-spatial behaviors, it is
416 unlikely that procedural errors contributed to the deficits described in the sections above.
417
418 **No-Platform Probe Test**
419 At each testing age, a no-platform probe test was conducted 24 hours after the
420 final day 5 training trial. Figure 10A shows heat maps representing the dwell time in each
421 location of the pool collapsed across animals in each of the Tg and WT groups. The heat
422 maps suggest that rats from each group organized their movements around the trained
423 platform location and spent a disproportionate amount of time near this region. To
424 determine whether the preference for the platform region is expressed for the full
425 duration of the probe session, we divided the analysis into four 15 second bins (Fig. 10B).
426 At each test age, measures of average proximity increased as a function of time bin,
427 suggesting that animals made fewer swims near the platform location by the end of each
428 probe session ($Fs\geq$ 3.30, $ps\leq$.025). However, measures of target preference score
429 indicated significant differences at 7-8 months of age only, whereby all animals had
430 significantly lower preference for the platform quadrant in the last 15s versus all other
431 time bins ($F(3,72)=3.132, p=.031$). Neither tests of proximity nor preference score
432 revealed significant Tg and sex differences or interaction effects at each test age,
433 indicating that groups displayed an equivalent search preference for the platform location
434 by the end of training.
435
436 **Morris Water Task - Cued Platform**
437 In the cued platform task, Tg and WT rats showed similar performance at each

testing age (Fig. S3). Mixed ANOVAs conducted on escape latencies at each time-point indicated all animals had decreased escape latencies in the second trial block versus the first trial block at 4-5 months and 7-5 months ($Fs \geq 4.46$, $ps \leq .0.045$), but only trending differences were observed at 10-11 months ($F(1,23)=3.81$, $p=.063$). Importantly, there were no group differences detected between Tg and WT groups at the three test ages. Further, there were no main effects of sex at each testing age. At 4-5 months of age, there was a significant sex by block effect, whereby female animals were slightly slower to reach the platform relative to male animals in the first trial block. Furthermore, Tg females had slightly elevated latencies to reach the platform relative to Tg males, though this genotype by sex effect only trended towards significance ($F(1,24)=2.97$,$p=.098$).

Discussion

The primary conclusion of the present study is that clear spatial navigation impairments by TgF344-AD rats were identified at 10-11 months of age. Specifically, TgF344-AD rats demonstrated increased escape latencies and path lengths, and they searched a wider area of the pool and were less precise in their search for the platform location (Figs 2 and 3). In addition, by 10-11 months of age, the directionality of their trajectories to the platform (Fig. 5 and 6) and switching from less direct to more direct trajectory types was attenuated in Tg rats (Fig. 8 and 9). While navigation impairments were detected during training in the hidden platform task, a 60 second no-platform probe test conducted on the 6th day indicated that both Tg and WT groups displayed a similar preference for the platform quadrant (Fig. 10). This pattern of impairments at 10-11 months supports the conclusion that although Tg animals are impaired at executing an

optimal trajectory and search pattern near the hidden platform region, Tg rats can express a preference for that location by the end of the experiment.

The deficits reported in the present study were observed in the absence of group differences in sensorimotor or procedural learning. Several analyses support this conclusion: first, measures of swim speed failed to indicate significant differences between Tg and WT groups at any age of testing. This observation is also consistent with recent work (Rorabaugh et al., 2017). Secondly, measures of non-spatial errors at each age of testing failed to indicate Tg and WT differences. Lastly, Tg and WT animals performed similarly on the cued platform task at each test age, indicating that Tg animals could learn to navigate by approaching a cue directly marking the goal. These findings strongly suggest that Tg and WT animals were equivalently capable of acquiring the non-spatial demands of the Morris water task.

The results of the present study offer some clarification regarding the time-course of spatial navigation impairment observed in this model. Only a small number of studies have investigated navigation in early stages of pathogenesis in the TgF344-AD model, with one study demonstrating clear deficits in the Morris water task at 6 months of age (Rorabaugh et al., 2017), and others showing largely intact navigation between 4 and 6 months (Cohen et al., 2013; Pentkowski et al., 2017). While the clearest navigation deficits were detected much later at 10-11 months of age in the present study, our results are also consistent with previous work in showing that Tg rats displayed a significant decrease in the directedness of their swim trajectories by 7 months of age. Notably, Tg and WT animals were equivalent in standard measures of water task performance at 7-8 months of age (i.e., escape latency and path length). One possible explanation for the

latter finding is that repeated spatial training and procedural learning may have allowed Tg animals to utilize strategies that result in similar performance on standard measures. Indeed, a convolution analysis indicated that Tg rats get better at less direct movements to find the platform than switching to more direct movements. Finally, it is important to note that previous studies report that Tg rats tend to have greater spatial difficulties in manipulations involving "reversal" tests in which the goal is moved to a novel location. Because Tg rats display intact navigation in standard tests at this age range (Cohen et al., 2013; Pentkowski et al., 2017; Rorabaugh et al., 2017), it is possible that reversal impairments may reflect the increasing demands on behavioral flexibility rather than navigation *per se*. This possibility should be explored in future work.

Overall, the spatial impairment in TgF344-AD rats found here also closely correspond to those observed in individuals with preclinical or prodromal AD (Guariglia and Nitrini, 2009; Pai and Jacobs, 2004). Although platform memory remained intact across all time points, Tg subjects exhibited less accurate trajectories and platform search patterns indicative of allocentric navigation impairments. In contrast, the intact cued platform navigation is suggestive of intact egocentric navigation. This pattern of impaired allocentric, and intact egocentric navigation, is consistent with impairments observed in human subjects with early AD (Serino et al., 2014). Thus, it is likely the preclinical phase of TgF344-AD rats lies prior to 10 months, and greater spatial navigation and memory impairment would be observed later. Prior characterization of pathological markers of AD in TgF344-AD rats supports this notion. Specifically, TgF344-AD rats develop neuropathic changes and entorhinal-to-hippocampus synaptic changes as early as 6 months of age (Cohen et al., 2013; Smith and McMahon, 2018) and neurovascular

dysfunction and CA3-to-CA1 synaptic changes at 9 months (Joo et al., 2017; Smith and McMahon, 2018), while significant amyloid plaques, inflammation, tauopathy and cell loss occurs at 16 months. Thus, the navigation differences observed at 10-11 months in TgF344-AD males could be considered a putative MCI phase, though further characterization of pathology and behavior is needed.

Although there were no clear differences between male and female Tg rats on measures of path length, platform proximity, or search area, we did observe a trend for greater escape latency at 10-11 months of age. Additionally, our detailed path analyses indicated that female Tg rats performed significantly fewer direct trajectories toward the hidden platform at 10-11 months of age. Interestingly, performance of direct paths by female Tg rats was similar at 7-8 and 10-11 months of age, suggesting a potential 7-month onset of subtle changes in swim path trajectory. Male Tg rats demonstrated a slightly decreased, yet apparent impairment, in direct navigation at 10-11 months. Thus, the attenuated directional deficits found in male Tg rats relative to female Tg rats may reflect sex-specific progression profiles like that found in various models of AD-like pathology (Clinton et al., 2007; Granger et al., 2016; King et al., 1999; Melnikova et al., 2016), and is consistent with human studies in which the prevalence and rate of conversion to AD is higher in females (Gao et al., 1998; Mielke et al., 2014; Pike, 2017) Finally, our observations suggest that detailed path analyses might have greater sensitivity at detecting group differences than general performance measures.

The hippocampus has been a strong focus in AD research, despite various other limbic circuit structural involvement in AD (Aggleton et al., 2016). Cohen and colleagues (2013) identified inflammation and initial tau changes at 6 months of age in the

529 hippocampus, and recent work has shown that this early expression of pathology also
530 impacts the medial entorhinal cortex and entorhinal-hippocampal synaptic plasticity
531 (Rorabaugh et al., 2017; Smith and McMahon, 2018). This coincides with the reported
532 early incidence of pathology in humans associated with the entorhinal cortex (Braak and
533 Braak, 1995), but fails to address whether TgF344-AD pathology emerges in other limbic
534 regions such as the anterior thalamic nuclei or retrosplenial cortex. This is particularly
535 important given cell types coding for head direction are found in both regions (Clark and
536 Taube, 2012; Taube, 2007), and damage to both regions can produce deficits in the
537 directional accuracy of navigation (Clark and Harvey, 2016; Harvey et al., 2017; Vann et
538 al., 2009). Whether TgF344-AD rats exhibit AD pathology and disrupted spatial
539 signaling in limbic-thalamic and limbic-cortical regions at early stages of development is
540 unknown and warrants investigation.
541
542 **Conclusions**
543 The present study found that TgF344-AD rats express clear navigation
544 impairments at 10-11 months of age. A detailed path analysis indicated that subtle
545 deficits in the directedness of trajectories to the hidden platform can be detected at earlier
546 ages and can be sensitive to sex differences. The latter observations may underlie the
547 subtle differences between Tg and WT rats that were found using classic measures of
548 water maze (escape latency, path length, search proximity and search area) at these ages,
549 and are likely not due to factors associated with non-spatial task demands. Furthermore,
550 spatial memory was intact for all animals across all ages indicating that developing
551 deficits observed at 10-11 months in Tg animals may be indicative of an MCI stage of

552 disease progression. Future work should identify whether the observed navigational
553 impairments in this model map onto brain regions involved in directional computation,
554 such as the anterior thalamus or retrosplenial cortex. Overall, the TgF344-AD rat model
555 provides substantial promise for elucidating neurobiological mechanisms of spatial
556 disorientation in AD.
557
558 Acknowledgments: This research was supported by grants from the Alzheimer's
559 Association (AARG-17-531572), NIGMS (P30GM103400), and an NM-INBRE
560 (P20GM10345). The authors thank Elizabeth Sneddon, John Madden, and Sara Benthem
561 for assistance with behavioral analysis and Dr. Derek Hamilton for technical support.
562
563 Disclosure: The authors declare that the research was conducted in the absence of any
564 commercial or financial relationships that could be construed as a potential conflict of
565 interest.

566 **References**

567 Aggleton, J.P., Pralus, A., Nelson, A.J.D., Hornberger, M., 2016. Thalamic pathology and
568 memory loss in early Alzheimer's disease: moving the focus from the medial
569 temporal lobe to Papez circuit. Brain 139, 1877–1890.
570 https://doi.org/10.1093/brain/aww083
571 Association, A., others, 2017. 2017 Alzheimer's disease facts and figures. Alzheimers
572 Dement. 13, 325–373.
573 Bianchini, F., Di Vita, A., Palermo, L., Piccardi, L., Blundo, C., Guariglia, C., 2014. A
574 Selective Egocentric Topographical Working Memory Deficit in the Early Stages
575 of Alzheimer's Disease: A Preliminary Study. Am. J. Alzheimers Dis. Dementiasr
576 29, 749–754. https://doi.org/10.1177/1533317514536597
577 Bird, C.M., Chan, D., Hartley, T., Pijnenburg, Y.A., Rossor, M.N., Burgess, N., 2010.
578 Topographical short-term memory differentiates Alzheimer's disease from
579 frontotemporal lobar degeneration. Hippocampus 20, 1154–1169.
580 https://doi.org/10.1002/hipo.20715
581 Braak, H., Braak, E., 1995. Staging of alzheimer's disease-related neurofibrillary
582 changes. Neurobiol. Aging, The Schmitt Symposium: The Cytoskeleton and
583 Alzheimer's Disease 16, 271–278. https://doi.org/10.1016/0197-4580(95)00021-6

584 Brody, D.L., Holtzman, D.M., 2006. Morris water maze search strategy analysis in
585 PDAPP mice before and after experimental traumatic brain injury. Exp. Neurol.
586 197, 330–340. https://doi.org/10.1016/j.expneurol.2005.10.020
587 Chan, D., Gallaher, L.M., Moodley, K., Minati, L., Burgess, N., Hartley, T., 2016. The 4
588 Mountains Test: A Short Test of Spatial Memory with High Sensitivity for the
589 Diagnosis of Pre-dementia Alzheimer's Disease. J. Vis. Exp. JoVE.
590 https://doi.org/10.3791/54454
591 Clark, B., Rice, J.P., Akers, K.G., Candelaria-Cook, F.T., Taube, J.S., Hamilton, D.A.,
592 2013. Lesions of the dorsal tegmental nuclei disrupt control of navigation by
593 distal landmarks in cued, directional, and place variants of the Morris water task.
594 Behav. Neurosci. 127, 566–581. https://doi.org/10.1037/a0033087
595 Clark, B.J., Harvey, R.E., 2016. Do the anterior and lateral thalamic nuclei make distinct
596 contributions to spatial representation and memory? Neurobiol. Learn. Mem. 133,
597 69–78. https://doi.org/10.1016/j.nlm.2016.06.002
598 Clark, B.J., Hong, N.S., Bettenson, D.J., Woolford, J., Horwood, L., McDonald, R.J.,
599 2015. Maintained directional navigation across environments in the Morris water
600 task is dependent on vestibular cues. J. Exp. Psychol. Anim. Learn. Cogn. 41,
601 301–308. https://doi.org/10.1037/xan0000066
602 Clark, B.J., Taube, J.S., 2012. Vestibular and attractor network basis of the head direction
603 cell signal in subcortical circuits. Front. Neural Circuits 6.
604 https://doi.org/10.3389/fncir.2012.00007
605 Clark, B.J., Taube, J.S., 2009. Deficits in landmark navigation and path integration after
606 lesions of the interpeduncular nucleus. Behav. Neurosci. 123, 490–503.
607 https://doi.org/10.1037/a0015477
608 Clinton, L.K., Billings, L.M., Green, K.N., Caccamo, A., Ngo, J., Oddo, S., McGaugh,
609 J.L., LaFerla, F.M., 2007. Age-dependent sexual dimorphism in cognition and
610 stress response in the 3xTg-AD mice. Neurobiol. Dis. 28, 76–82.
611 https://doi.org/10.1016/j.nbd.2007.06.013
612 Cohen, R.M., Rezai-Zadeh, K., Weitz, T.M., Rentsendorj, A., Gate, D., Spivak, I.,
613 Bholat, Y., Vasilevko, V., Glabe, C.G., Breunig, J.J., Rakic, P., Davtyan, H.,
614 Agadjanyan, M.G., Kepe, V., Barrio, J.R., Bannykh, S., Szekely, C.A., Pechnick,
615 R.N., Town, T., 2013. A Transgenic Alzheimer Rat with Plaques, Tau Pathology,
616 Behavioral Impairment, Oligomeric A , and Frank Neuronal Loss. J. Neurosci. 33,
617 6245–6256. https://doi.org/10.1523/JNEUROSCI.3672-12.2013
618 Cushman, L.A., Stein, K., Duffy, C.J., 2008. Detecting navigational deficits in cognitive
619 aging and Alzheimer disease using virtual reality. Neurology 71, 888–895.
620 https://doi.org/10.1212/01.wnl.0000326262.67613.fe
621 deIpolyi, A.R., Rankin, K.P., Mucke, L., Miller, B.L., Gorno-Tempini, M.L., 2007.
622 Spatial cognition and the human navigation network in AD and MCI. Neurology
623 69, 986–997. https://doi.org/10.1212/01.wnl.0000271376.19515.c6
624 Do Carmo, S., Cuello, A.C., 2013. Modeling Alzheimer's disease in transgenic rats. Mol.
625 Neurodegener. 8, 37.
626 Dubois, B., Padovani, A., Scheltens, P., Rossi, A., Dell'Agnello, G., 2016. Timely
627 Diagnosis for Alzheimer's Disease: A Literature Review on Benefits and
628 Challenges. J. Alzheimers Dis. JAD 49, 617–631. https://doi.org/10.3233/JAD-
629 150692

630 Gallagher, M., Burwell, R., Burchinal, M., 1993. Severity of spatial learning impairment
631 in aging: development of a learning index for performance in the Morris water
632 maze. Behav. Neurosci. 107, 618–626.
633 Gao, S., Hendrie, H.C., Hall, K.S., Hui, S., 1998. The relationships between age, sex, and
634 the incidence of dementia and Alzheimer disease: a meta-analysis. Arch. Gen.
635 Psychiatry 55, 809–815.
636 Garthe, A., Behr, J., Kempermann, G., 2009. Adult-Generated Hippocampal Neurons
637 Allow the Flexible Use of Spatially Precise Learning Strategies. PLoS ONE 4.
638 https://doi.org/10.1371/journal.pone.0005464
639 Gehring, T.V., Luksys, G., Sandi, C., Vasilaki, E., 2015. Detailed classification of
640 swimming paths in the Morris Water Maze: multiple strategies within one trial.
641 Sci. Rep. 5. https://doi.org/10.1038/srep14562
642 Graham, W.V., Bonito-Oliva, A., Sakmar, T.P., 2017. Update on Alzheimer's Disease
643 Therapy and Prevention Strategies. Annu. Rev. Med. 68, 413–430.
644 https://doi.org/10.1146/annurev-med-042915-103753
645 Granger, M.W., Franko, B., Taylor, M.W., Messier, C., George-Hyslop, P.S., Bennett,
646 S.A.L., 2016. A TgCRND8 Mouse Model of Alzheimer's Disease Exhibits
647 Sexual Dimorphisms in Behavioral Indices of Cognitive Reserve. J. Alzheimers
648 Dis. 51, 757–773. https://doi.org/10.3233/JAD-150587
649 Graziano, A., Petrosini, L., Bartoletti, A., 2003. Automatic recognition of explorative
650 strategies in the Morris water maze. J. Neurosci. Methods 130, 33–44.
651 https://doi.org/10.1016/S0165-0270(03)00187-0
652 Guariglia, C.C., Nitrini, R., 2009. Topographical disorientation in Alzheimer's disease.
653 Arq. Neuropsiquiatr. 67, 967–972.
654 Harker, K.T., Whishaw, I.Q., 2002. Impaired spatial performance in rats with
655 retrosplenial lesions: importance of the spatial problem and the rat strain in
656 identifying lesion effects in a swimming pool. J. Neurosci. Off. J. Soc. Neurosci.
657 22, 1155–1164.
658 Harvey, R.E., Thompson, S.M., Sanchez, L.M., Yoder, R.M., Clark, B.J., 2017. Post-
659 training Inactivation of the Anterior Thalamic Nuclei Impairs Spatial Performance
660 on the Radial Arm Maze. Front. Neurosci. 11.
661 https://doi.org/10.3389/fnins.2017.00094
662 Hort, J., Laczó, J., Vyhnálek, M., Bojar, M., Bureš, J., Vlček, K., 2007. Spatial
663 navigation deficit in amnestic mild cognitive impairment. Proc. Natl. Acad. Sci.
664 104, 4042–4047.
665 Joo, I.L., Lai, A.Y., Bazzigaluppi, P., Koletar, M.M., Dorr, A., Brown, M.E., Thomason,
666 L.A.M., Sled, J.G., McLaurin, J., Stefanovic, B., 2017. Early neurovascular
667 dysfunction in a transgenic rat model of Alzheimer's disease. Sci. Rep. 7, 46427.
668 https://doi.org/10.1038/srep46427
669 King, D.L., Arendash, G.W., Crawford, F., Sterk, T., Menendez, J., Mullan, M.J., 1999.
670 Progressive and gender-dependent cognitive impairment in the APPSW
671 transgenic mouse model for Alzheimer's disease. Behav. Brain Res. 103, 145–
672 162. https://doi.org/10.1016/S0166-4328(99)00037-6
673 Laczó, J., Vlček, K., Vyhnálek, M., Vajnerová, O., Ort, M., Holmerová, I., Tolar, M.,
674 Andel, R., Bojar, M., Hort, J., 2009. Spatial navigation testing discriminates two

types of amnestic mild cognitive impairment. Behav. Brain Res. 202, 252–259. https://doi.org/10.1016/j.bbr.2009.03.041

LaFerla, F.M., Green, K.N., 2012. Animal Models of Alzheimer Disease. Cold Spring Harb. Perspect. Med. 2. https://doi.org/10.1101/cshperspect.a006320

Melnikova, T., Park, D., Becker, L., Lee, D., Cho, E., Sayyida, N., Tian, J., Bandeen-Roche, K., Borchelt, D.R., Savonenko, A.V., 2016. Sex-related dimorphism in dentate gyrus atrophy and behavioral phenotypes in an inducible tTa:APPsi transgenic model of Alzheimer's disease. Neurobiol. Dis. 96, 171–185. https://doi.org/10.1016/j.nbd.2016.08.009

Mielke, M.M., Vemuri, P., Rocca, W.A., 2014. Clinical epidemiology of Alzheimer's disease: assessing sex and gender differences. Clin. Epidemiol. 6, 37–48. https://doi.org/10.2147/CLEP.S37929

Monacelli, A.M., Cushman, L.A., Kavcic, V., Duffy, C.J., 2003. Spatial disorientation in Alzheimer's disease: the remembrance of things passed. Neurology 61, 1491–1497. https://doi.org/10.1212/WNL.61.11.1491

Morganti, F., Stefanini, S., Riva, G., 2013. From allo- to egocentric spatial ability in early Alzheimer's disease: a study with virtual reality spatial tasks. Cogn. Neurosci. 4, 171–180. https://doi.org/10.1080/17588928.2013.854762

Morris, R., 1984. Developments of a water-maze procedure for studying spatial learning in the rat. J. Neurosci. Methods 11, 47–60.

Pai, M.-C., Jacobs, W.J., 2004. Topographical disorientation in community-residing patients with Alzheimer's disease. Int. J. Geriatr. Psychiatry 19, 250–255. https://doi.org/10.1002/gps.1081

Pentkowski, N.S., Berkowitz, L.E., Thompson, S.M., Drake, E.N., Olguin, C.R., Clark, B.J., 2017. Anxiety-like behavior as an early endophenotype in the TgF344-AD rat model of Alzheimer's disease. Neurobiol. Aging 61, 169–176. https://doi.org/10.1016/j.neurobiolaging.2017.09.024

Petersen, R.C., 2004. Mild cognitive impairment as a diagnostic entity. J. Intern. Med. 256, 183–194. https://doi.org/10.1111/j.1365-2796.2004.01388.x

Pike, C.J., 2017. Sex and the development of Alzheimer's disease. J. Neurosci. Res. 95, 671–680. https://doi.org/10.1002/jnr.23827

Rorabaugh, J.M., Chalermpalanupap, T., Botz-Zapp, C.A., Fu, V.M., Lembeck, N.A., Cohen, R.M., Weinshenker, D., 2017. Chemogenetic locus coeruleus activation restores reversal learning in a rat model of Alzheimer's disease. Brain 140, 3023–3038. https://doi.org/10.1093/brain/awx232

Ruediger, S., Spirig, D., Donato, F., Caroni, P., 2012. Goal-oriented searching mediated by ventral hippocampus early in trial-and-error learning. Nat. Neurosci. 15, 1563–1571. https://doi.org/10.1038/nn.3224

Saucier, D., Cain, D.P., 1995. Spatial learning without NMDA receptor-dependent long-term potentiation. Nature 378, 186–189. https://doi.org/10.1038/378186a0

Saucier, D., Hargreaves, E.L., Boon, F., Vanderwolf, C.H., Cain, D.P., 1996. Detailed behavioral analysis of water maze acquisition under systemic NMDA or muscarinic antagonism: Nonspatial pretraining eliminates spatial learning deficits. Behav. Neurosci. 110, 103–116. https://doi.org/10.1037/0735-7044.110.1.103

719 Serino, S., Cipresso, P., Morganti, F., Riva, G., 2014. The role of egocentric and
720 allocentric abilities in Alzheimer's disease: a systematic review. Ageing Res. Rev.
721 16, 32–44. https://doi.org/10.1016/j.arr.2014.04.004
722 Smith, L.A., McMahon, L.L., 2018. Deficits in synaptic function occur at medial
723 perforant path-dentate granule cell synapses prior to Schaffer collateral-CA1
724 pyramidal cell synapses in the novel TgF344-Alzheimer's Disease Rat Model.
725 Neurobiol. Dis. 110, 166–179. https://doi.org/10.1016/j.nbd.2017.11.014
726 Stone, S.S.D., Teixeira, C.M., DeVito, L.M., Zaslavsky, K., Josselyn, S.A., Lozano,
727 A.M., Frankland, P.W., 2011. Stimulation of Entorhinal Cortex Promotes Adult
728 Neurogenesis and Facilitates Spatial Memory. J. Neurosci. 31, 13469–13484.
729 https://doi.org/10.1523/JNEUROSCI.3100-11.2011
730 Taube, J.S., 2007. The Head Direction Signal: Origins and Sensory-Motor Integration.
731 Annu. Rev. Neurosci. 30, 181–207.
732 https://doi.org/10.1146/annurev.neuro.29.051605.112854
733 Thal, D.R., Rüb, U., Orantes, M., Braak, H., 2002. Phases of Aβ-deposition in the human
734 brain and its relevance for the development of Ad. Neurology 58, 1791–1800.
735 https://doi.org/10.1212/WNL.58.12.1791
736 Tu, S., Wong, S., Hodges, J.R., Irish, M., Piguet, O., Hornberger, M., 2015. Lost in
737 spatial translation – A novel tool to objectively assess spatial disorientation in
738 Alzheimer's disease and frontotemporal dementia. Cortex 67, 83–94.
739 https://doi.org/10.1016/j.cortex.2015.03.016
740 van Groen, T., Kadish, I., Wyss, J.M., 2002. Old rats remember old tricks; memories of
741 the water maze persist for 12 months. Behav. Brain Res. 136, 247–255.
742 Vann, S., P Aggleton, J., A Maguire, E., 2009. What does the retrosplenial cortex do?
743 https://doi.org/10.1038/nrn2733
744 Vicens, P., Redolat, R., Carrasco, M.C., 2002. Effects of early spatial training on water
745 maze performance: a longitudinal study in mice. Exp. Gerontol. 37, 575–581.
746 Voorhees, J.R., Remy, M.T., Cintrón-Pérez, C.J., El Rassi, E., Khan, M.Z., Dutca, L.M.,
747 Yin, T.C., McDaniel, L.N., Williams, N.S., Brat, D.J., Pieper, A.A., 2017. (−)-
748 P7C3-S243 Protects a Rat Model of Alzheimer's Disease From Neuropsychiatric
749 Deficits and Neurodegeneration Without Altering Amyloid Deposition or
750 Reactive Glia. Biol. Psychiatry. https://doi.org/10.1016/j.biopsych.2017.10.023
751 Vorhees, C.V., Williams, M.T., 2014. Assessing spatial learning and memory in rodents.
752 ILAR J. 55, 310–332. https://doi.org/10.1093/ilar/ilu013
753 Vorhees, C.V., Williams, M.T., 2006. Morris water maze: procedures for assessing
754 spatial and related forms of learning and memory. Nat. Protoc. 1, 848–858.
755 https://doi.org/10.1038/nprot.2006.116
756 Winblad, B., Palmer, K., Kivipelto, M., Jelic, V., Fratiglioni, L., Wahlund, L.-O.,
757 Nordberg, A., Bäckman, L., Albert, M., Almkvist, O., Arai, H., Basun, H.,
758 Blennow, K., de Leon, M., DeCarli, C., Erkinjuntti, T., Giacobini, E., Graff, C.,
759 Hardy, J., Jack, C., Jorm, A., Ritchie, K., van Duijn, C., Visser, P., Petersen, R.C.,
760 2004. Mild cognitive impairment--beyond controversies, towards a consensus:
761 report of the International Working Group on Mild Cognitive Impairment. J.
762 Intern. Med. 256, 240–246. https://doi.org/10.1111/j.1365-2796.2004.01380.x

763 Wolfer, D.P., Lipp, H.P., 2000. Dissecting the behaviour of transgenic mice: is it the
764 mutation, the genetic background, or the environment? Exp. Physiol. 85, 627–
765 634.
766 Yew, B., Alladi, S., Shailaja, M., Hodges, J.R., Hornberger, M., 2013. Lost and
767 forgotten? Orientation versus memory in Alzheimer's disease and frontotemporal
768 dementia. J. Alzheimers Dis. JAD 33, 473–481. https://doi.org/10.3233/JAD-
769 2012-120769
770

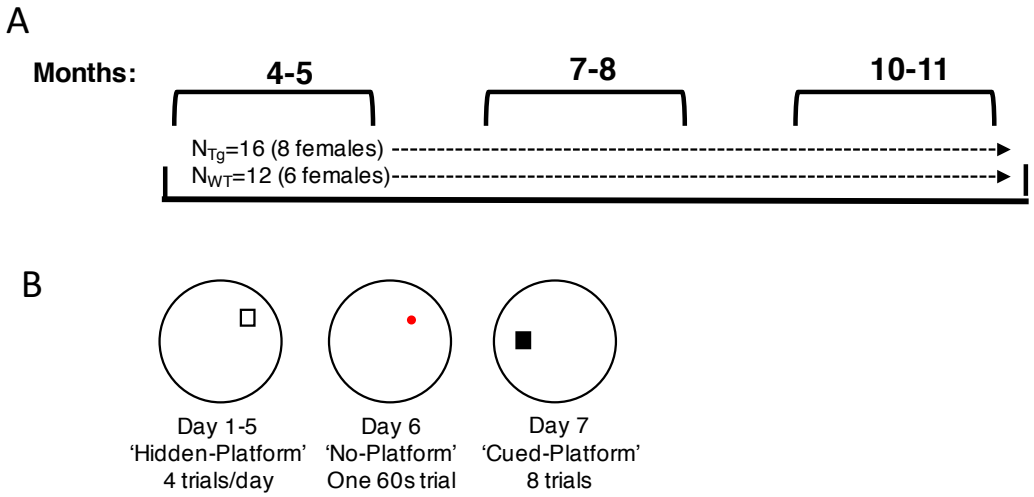

Figure 1. Study Time line. (A) TgF344-AD (n=16) and wild-type F344 rats (n=12) underwent testing at three age points (shown in months). (B) The temporal order of testing consisted of 5 days of training followed by a no-platform probe trial and finally a cued-platform test on day 7. White square=hidden platform, red circle=prior platform area, black square= cued-platform.

771
772

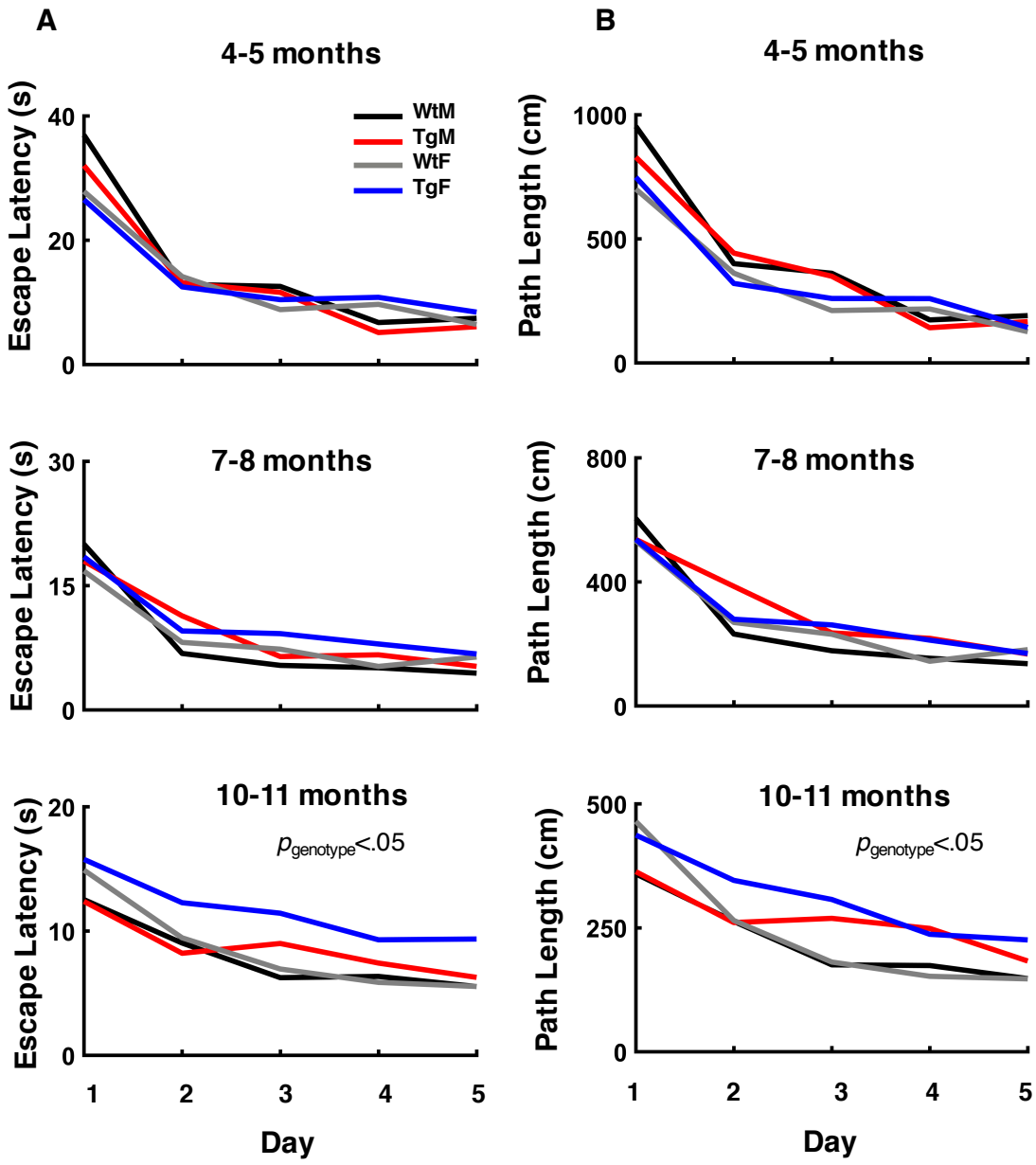

Figure 2. TgF344-AD rats took more time to reach the platform and had longer path lengths during hidden-platform training compared to WT controls starting at 10-11 months of age. (A) Mean escape Latency in seconds plotted over days at all age points. Main effect of genotype observed at 10-11months, (p<.05, Mixed ANOVA). (B) Mean path length in centimeters plotted over days at all age points. Main effect of genotype observed at 10-11months, (p<.05, Mixed ANOVA). Groups distinguished by color: black=Wild Type males (WtM), red=Transgenic males (TgM), gray=Wild Type females (WtF), blue=Transgenic females (TgF).

773
774

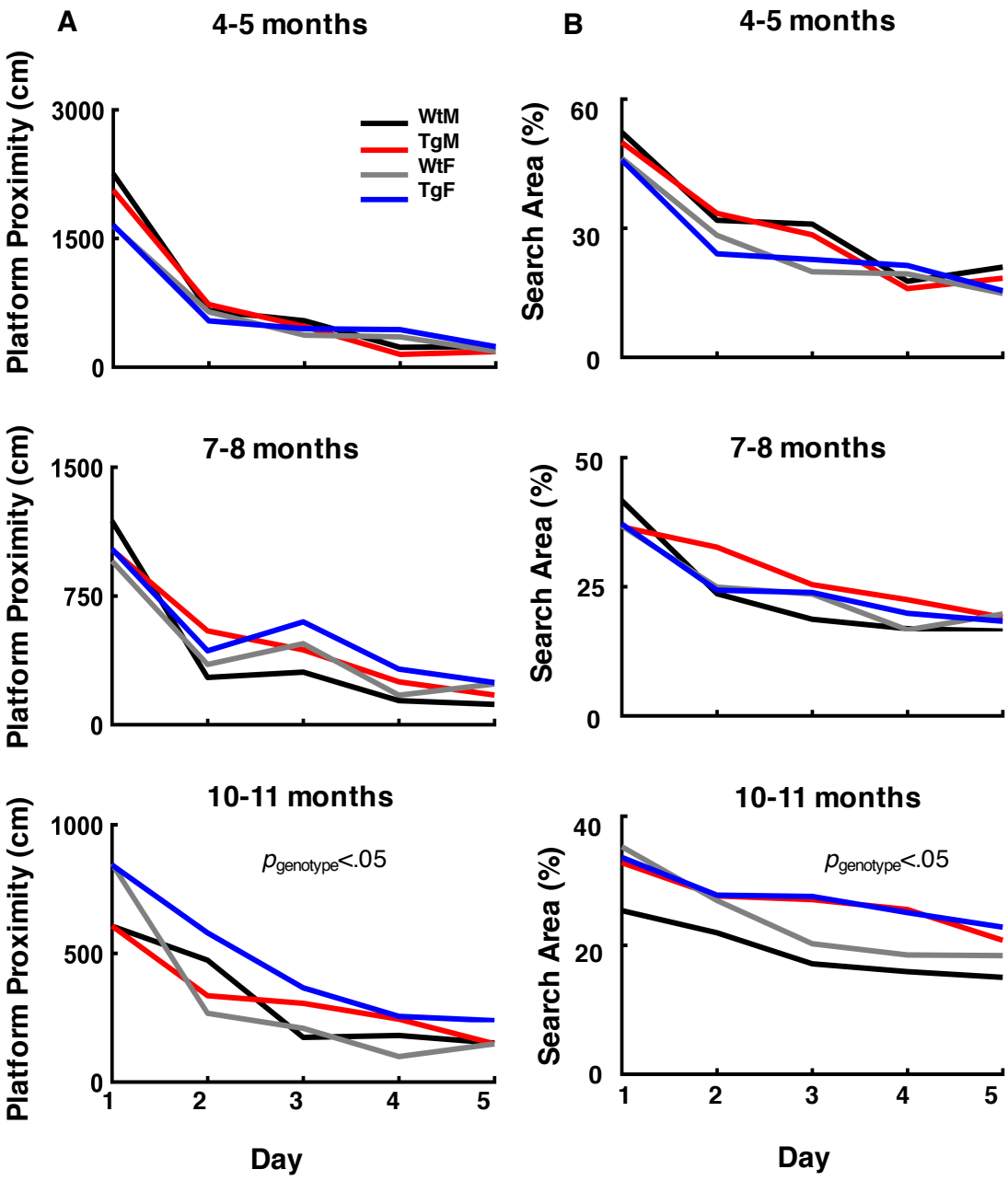

Figure 3. During hidden-platform training, TgF344-AD rats swam further from the platform and swam a larger proportion of the pool area relative to WT controls starting at 10-11 months of age. (A) Mean platform proximity in centimeters plotted over days at all age points. Main effect of genotype observed at 10-11months, (p<.05, Mixed ANOVA). (B) Percentage of search area explored plotted over days at all age points. Main effect of genotype observed at 10-11months, (p<.05, Mixed ANOVA). Groups distinguished by color: black=Wild Type males (WtM), red=Transgenic males (TgM), gray=Wild Type females (WtF), blue=Transgenic females (TgF).

775
776

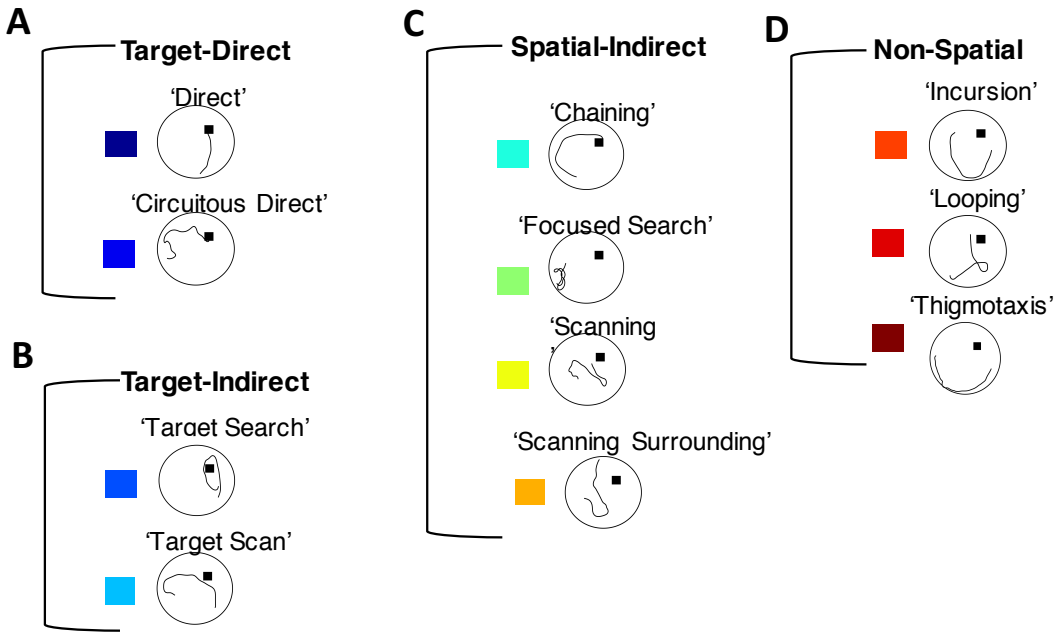

Figure 4. Representative examples of individual swim segments. (A) Target-direct (platform found within first segment). (B) Target-indirect (area around platform searched). (C) Spatial-indirect (spatial components not directed at platform). (D) Non-spatial (limited spatial components). See *Methods* for operational definitions of individual strategies.

777

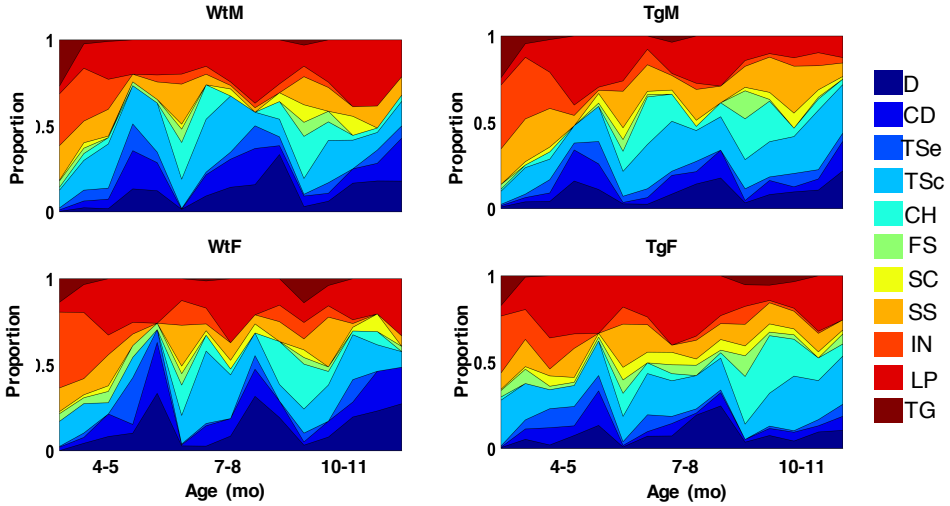

Figure 5. Relative proportion of swim strategies over days at each age of testing. Area plots showing the proportion of all strategies across days and age points. Colors indicate strategies, D=Direct, CD=Circuitous Direct, TSe=Target Search, TSc=Target Scan, CH=Chaining, FS=Focused Search, SC=Scanning, SS=Scanning Surroundings, IN=Incursion, LP=Looping, TG=Thigmotaxis. Note that Tg animals show fewer direct (D) and circuitous-direct (CD) compared to WT at 7-8 months and 10-11 months of age.

778
779

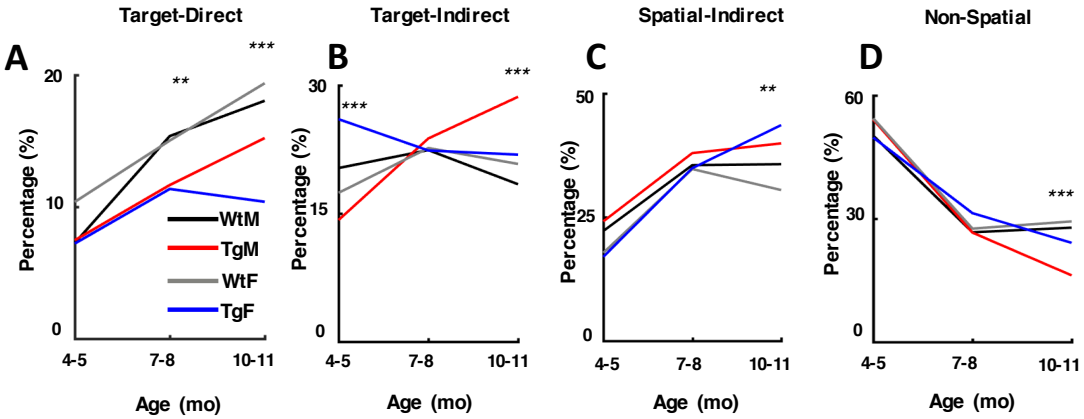

Figure 6. Line plots indicating the percentage of Target-Direct (A), Target-Indirect (B), Spatial-Indirect (C) and Non-Spatial (D) categories across ages. Note that Tg animals show a lower percentage of Target-Direct strategies starting at 7-8mo of age. Tg Males have a significantly higher proportion of Target-Indirect strategies at 10-11mo while Tg females use Spatial-Indirect strategies to a greater extent than WT females at 10-11mo. Tg animals show less Non-Spatial swim strategies compared to WT at 10-11 months (**p*<.05; ***p*<.01; ****p*<.001).

780
781

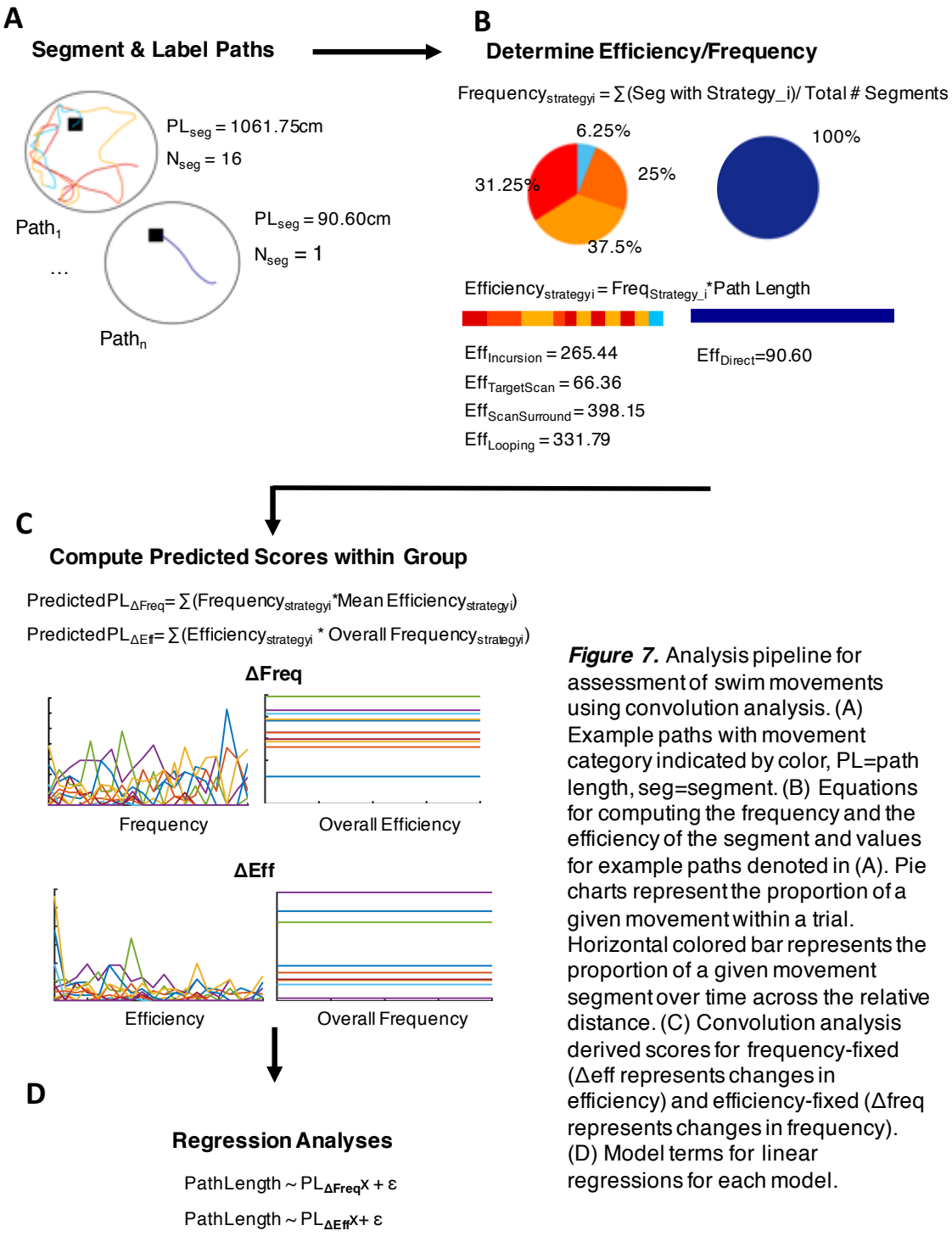

Figure 7. Analysis pipeline for assessment of swim movements using convolution analysis. (A) Example paths with movement category indicated by color, PL=path length, seg=segment. (B) Equations for computing the frequency and the efficiency of the segment and values for example paths denoted in (A). Pie charts represent the proportion of a given movement within a trial. Horizontal colored bar represents the proportion of a given movement segment over time across the relative distance. (C) Convolution analysis derived scores for frequency-fixed (Δeff represents changes in efficiency) and efficiency-fixed (Δfreq represents changes in frequency). (D) Model terms for linear regressions for each model.

782

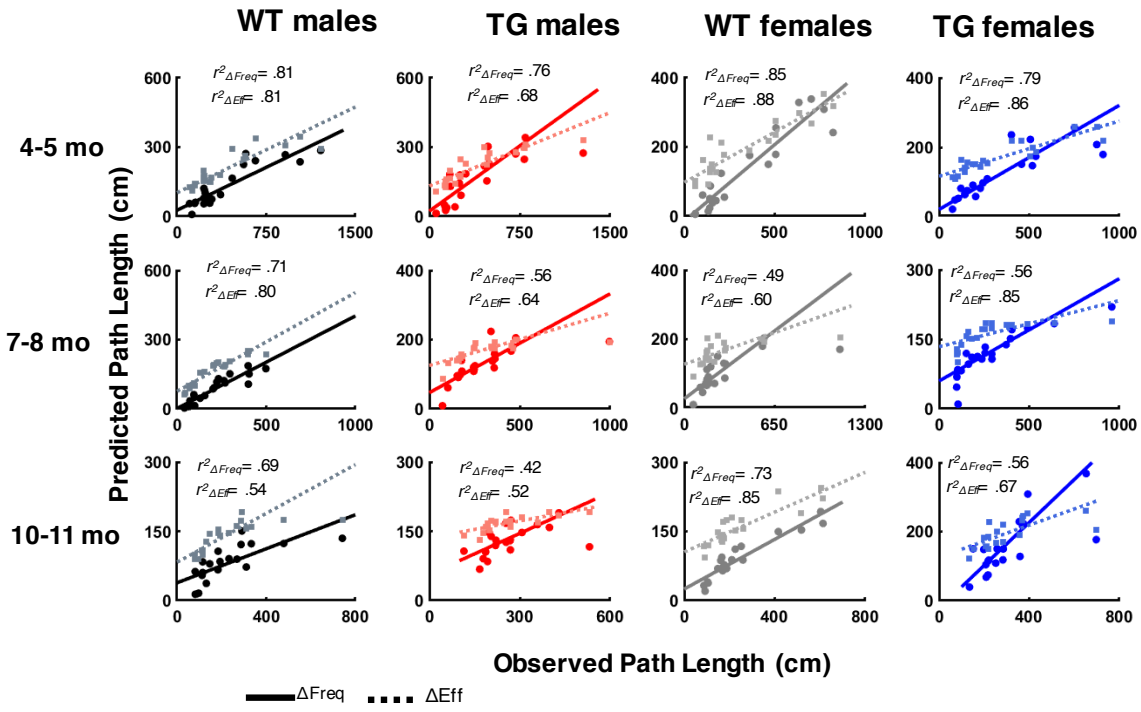

Figure 8. Scatter plots of derived predicted path length (cm) and observed path length (cm). Changing between movements (solid line) and their efficiency (dashed line) was significantly predictive of performance for all animals at each age of testing.

783
784

		4-5mo			7-8mo			10-11mo		
Model	Model	β	p	r^2	β	p	r^2	β	p	r^2
Δeff	WT Males	2.24	***	.81	1.97	***	.80	1.86	***	.54
	TG Males	1.96	***	.68	2.24	***	.64	1.80	**	.45
	WT Females	2.99	***	.86	1.37	**	.60	2.75	***	.85
	TG Females	1.93	***	.89	3.57	***	.85	.993	***	.67
Δfreq	WT Males	3.21	***	.82	2.02	***	.71	2.32	***	.69
	TG Males	3.16	***	.77	3.77	***	.56	4.12	***	.52
	WT Females	2.95	***	.85	1.40	n.s	.49	3.01	***	.74
	TG Females	4.79	***	.79	3.66	***	.56	1.76	***	.56

Figure 9. Linear regressions indicate dynamic patterns of swim movements across testing age. Δeff= regression model of predicted score computed by allowing efficiency to modulate over trials (i.e. frequency-fixed). Δfreq = regression model of predicted scores computed allowing frequency to modulate over trials (i.e. efficiency-fixed). $^{**}p<.01$, $^{***}p<.001$.

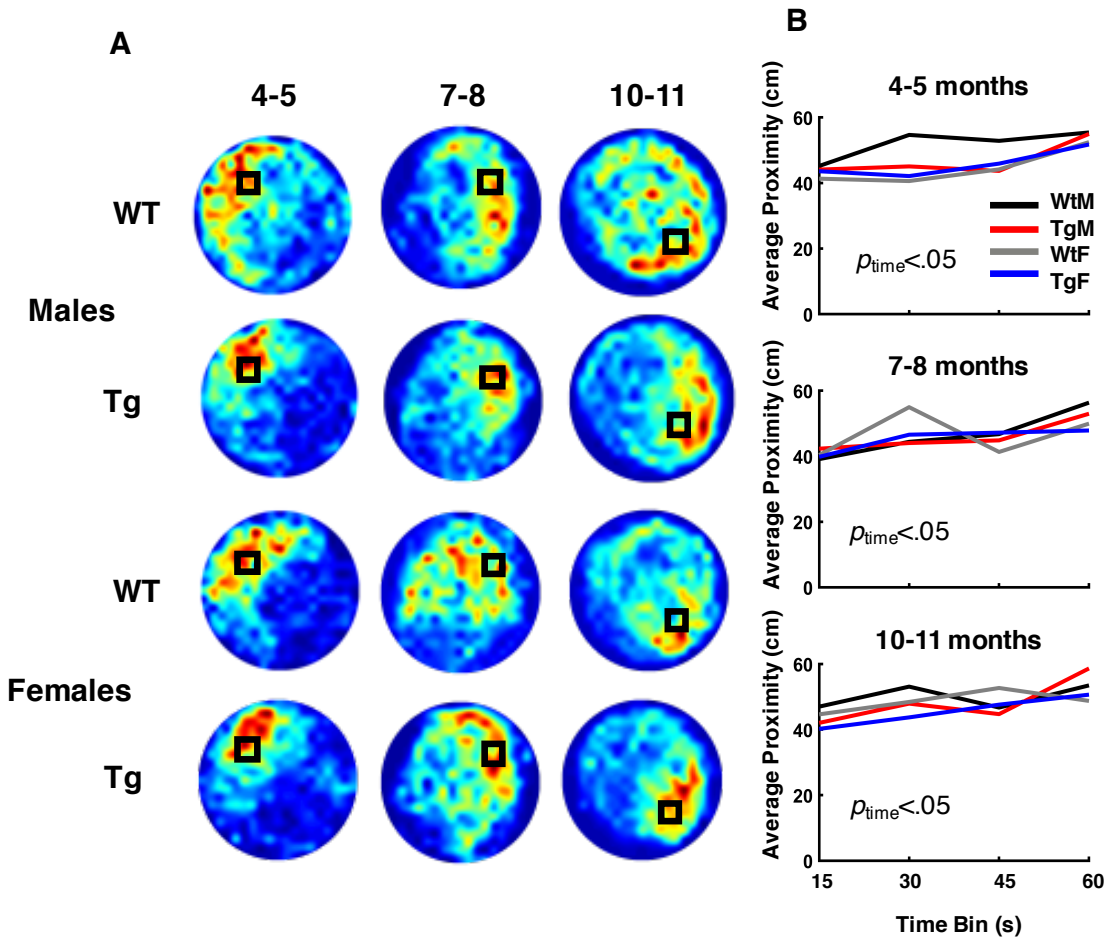

Figure 10. All groups exhibited similar preference for the platform location during the probe trial. (A) Heat maps represent weighted occupancy across entire 60s trial. Hot colors indicate longer dwell times. The platform area is denoted with a black square. (B) Average proximity away from the platform in centimeters is plotted across 15s time bins. All groups demonstrated similar average proximity within each time bin, though proximity to the platform increased as function of time (p<.05, Mixed ANOVA).

787

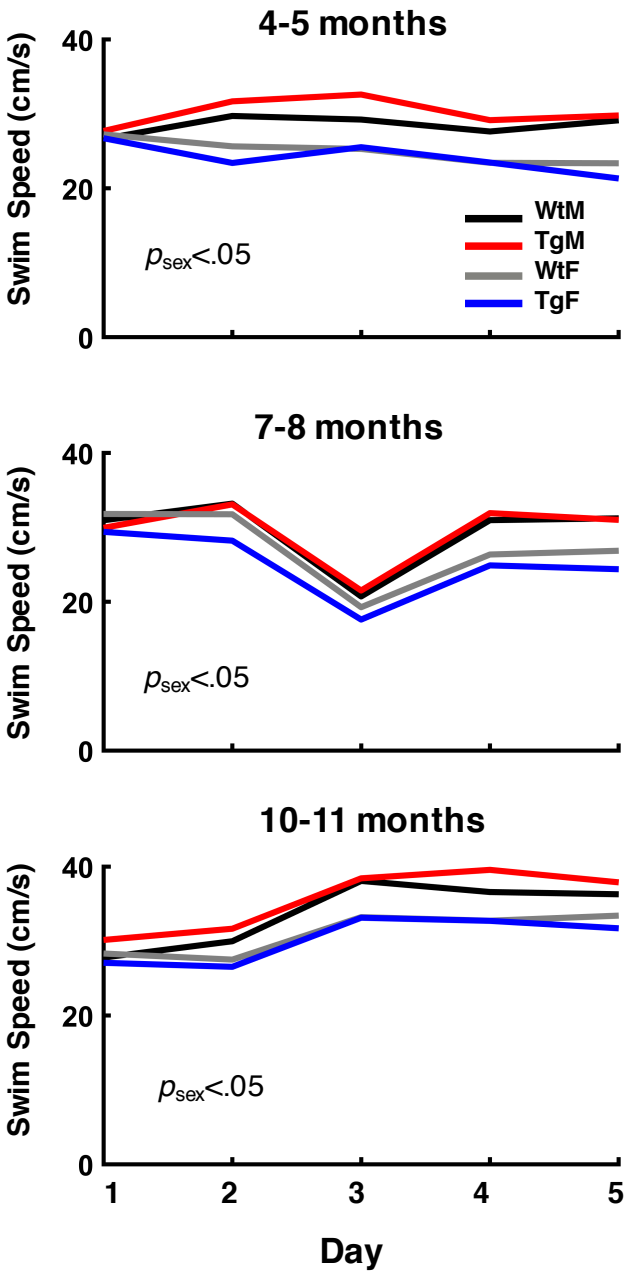

Figure S1. Average swim speed (cm/s) is plotted for each age of testing. Groups distinguished by color: black=Wild Type males (WtM), red=Transgenic males (TgM), gray=Wild Type females (WtF), blue=Transgenic females (TgF). Note that males consistently swam faster than females across all age points (ps<.05, ANOVAs).

788
789

	4-5mo		7-8mo		10-11mo	
	Mean	*SEM*	*Mean*	*SEM*	*Mean*	*SEM*
WT Males	.030	±.002	.050	±.003	.070	±.001
Tg+/- Males	.081	±.002	.043	±.001	.081	±.002
WT Females	.100	±.001	.083	±.004	.042	±.002
Tg+/- Females	.044	±.002	.025	±.001	.070	±.002

Figure S2. Table showing the means and SEM on non-spatial errors at each age of testing

790
791

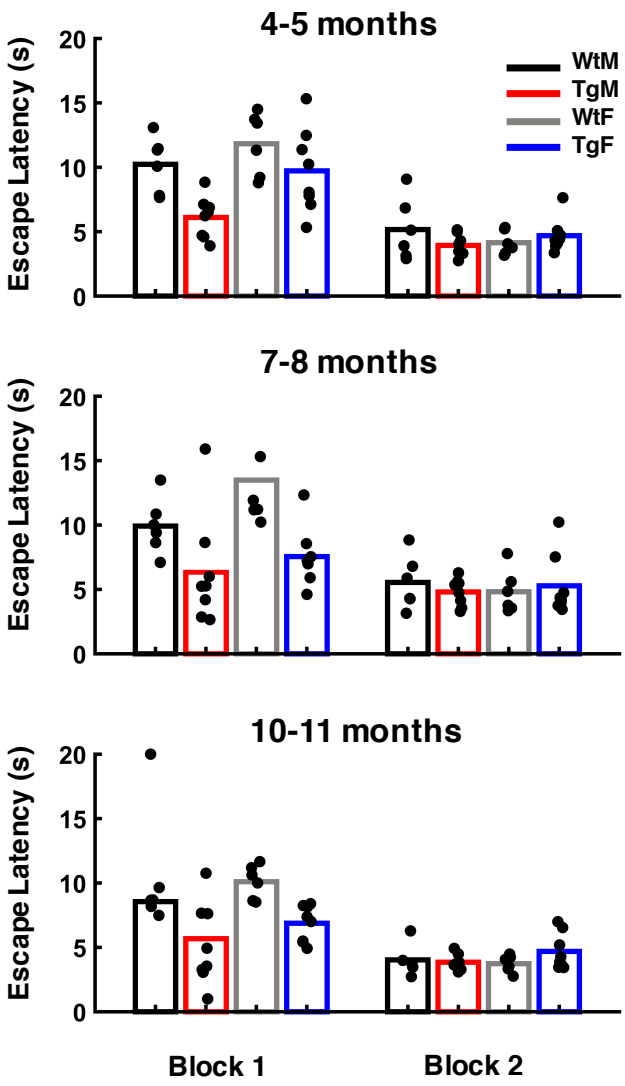

Figure S3. Mean escape latency (s) across trial blocks (set of 4 trials per block) during cued task was not different between groups at each age of testing. Mean latencies are plotted for each animal (black circles) to show distribution. Groups distinguished by color: black=Wild Type males (WtM), red=Transgenic males (TgM), gray=Wild Type females (WtF), blue=Transgenic females (TgF).

792